ORIGINAL RESEARCH

# Novel L-(CaP-ZnP)/SA Nanocomposite Hydrogel with Dual Anti-Inflammatory and Mineralization Effects for Efficient Vital Pulp Therapy

Xu Zhang[1,*], Xue Zhou[2,*], Wenhao Zhai[1,*], Jing Cui[1], Ziyi Pan[1], Liuyi Du[1], Linlin Wen[1], Rongrong Ye[1], Boya Zhang[1], Lei Huang[1], Daowei Li[1], Chungang Wang[2], Hongchen Sun [1]

[1]Jilin Provincial Key Laboratory of Tooth Development and Bone Remodeling, Hospital of Stomatology, Jilin University, Changchun, 130021, People's Republic of China; [2]Department of Chemistry, Northeast Normal University, Changchun, 130024, People's Republic of China

*These authors contributed equally to this work

Correspondence: Daowei Li; Lei Huang, Email jluldw@jlu.edu.cn; huanglei17@mails.jlu.edu.cn

**Background:** Vital pulp therapy (VPT) is considered a conservative treatment for preserving pulp viability in caries and trauma-induced pulpitis. However, Mineral trioxide aggregate (MTA) as the most frequently used repair material, exhibits limited efficacy under inflammatory conditions. This study introduces an innovative nanocomposite hydrogel, tailored to simultaneously target anti-inflammation and dentin mineralization, aiming to efficiently preserve vital pulp tissue.

**Methods:** The L-(CaP-ZnP)/SA nanocomposite hydrogel was designed by combining L-Arginine modified calcium phosphate/zinc phosphate nanoparticles (L-(CaP-ZnP) NPs) with sodium alginate (SA), and was characterized with TEM, SEM, FTIR, EDX, ICP–AES, and Zeta potential. In vitro, we evaluated the cytotoxicity and anti-inflammatory properties. Human dental pulp stem cells (hDPSCs) were cultured with lipopolysaccharide (LPS) to induce an inflammatory response, and the cell odontogenic differentiation was measured and possible signaling pathways were explored by alkaline phosphatase (ALP)/alizarin red S (ARS) staining, qRT-PCR, immunofluorescence staining, and Western blotting, respectively. In vivo, a pulpitis model was utilized to explore the potential of the L-(CaP-ZnP)/SA nanocomposite hydrogel in controlling pulp inflammation and enhancing dentin mineralization by Hematoxylin and eosin (HE) staining and immunohistochemistry staining.

**Results:** In vitro experiments revealed that the nanocomposite hydrogel was synthesized successfully and presented desirable biocompatibility. Under inflammatory conditions, compared to MTA, the L-(CaP-ZnP)/SA nanocomposite hydrogel demonstrated superior anti-inflammatory and pro-odontogenesis effects. Furthermore, the nanocomposite hydrogel significantly augmented p38 phosphorylation, implicating the involvement of the p38 signaling pathway in pulp repair. Significantly, in a rat pulpitis model, the L-(CaP-ZnP)/SA nanocomposite hydrogel downregulated inflammatory markers while upregulating mineralization-related markers, thereby stimulating the formation of robust reparative dentin.

**Conclusion:** The L-(CaP-ZnP)/SA nanocomposite hydrogel with good biocompatibility efficiently promoted inflammation resolution and enhanced dentin mineralization by activating p38 signal pathway, as a pulp-capping material, offering a promising and advanced solution for treatment of pulpitis.

**Keywords:** nanocomposite hydrogel, vital pulp therapy, pulpitis, p38 signaling pathway

## Introduction

Maintaining dental pulp vitality stands as a crucial factor in preserving tooth nutrition and sensation. The onset of caries or dental trauma can trigger pulp inflammation, potentially progressing to irreversible pulpitis and eventual necrosis.[1,2] While conventional root canal therapy (RCT) serves as the primary treatment modality for pulpitis, its application poses risks to tooth integrity, leading to a loss of dental pulp vitality and essential functions. Consequently, RCT could result in permanent devitalization of the tooth, rendering it fragile and susceptible to reinfection and fractures.[3,4]

**Graphical Abstract**
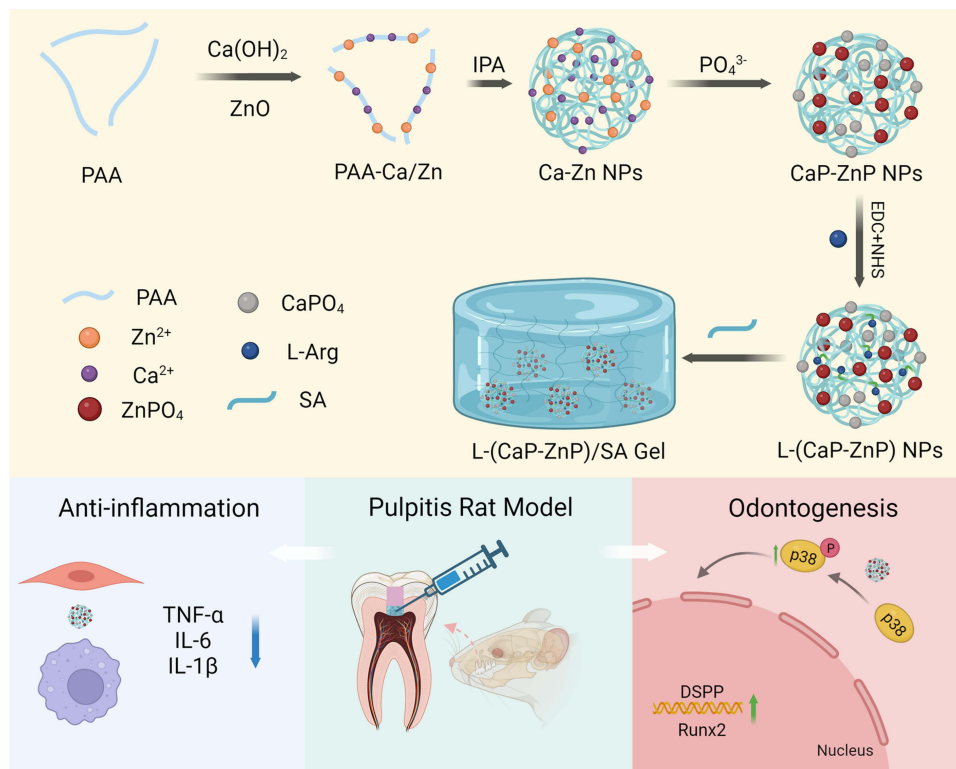


Vital pulp therapy (VPT) represents an integral facet in the conservation of healthy pulp tissue, sustaining pulp vitality, fostering restorative dentin formation, and upholding normal physiological tooth functions. Aligned with the ethos of minimally invasive treatment, VPT stands as a pivotal developmental trajectory in contemporary dental pulp therapy.[5] Notably, treatment modalities for VPT primarily encompass pulp capping and pulpotomy.[6] Presently, Mineral Trioxide Aggregate (MTA) reigns as the prevailing clinical material for pulp-capping agents, considered the gold standard in clinical practice.[7] Composed of micro hydrophilic particles, MTA comprises key compounds such as tricalcium oxide, tricalcium silicate, tricalcium aluminate, and silicate oxide.[8] Upon interaction with exudates, MTA undergoes a transformation into calcium hydroxide, thereby instigating the stimulation of hard tissue repair processes.[9] Despite its prevalent use, MTA exhibits limited efficacy in mitigating inflammatory responses. When utilized as a pulp-capping agent within inflamed pulpal tissues, MTA demonstrates compromised odontogenic differentiation and incomplete pulp healing, potentially culminating in pulp capping failures.[10] Consequently, exploring novel pulp-capping materials capable of concurrently exerting potent anti-inflammatory effects while fostering the formation of restorative dentin assumes paramount clinical significance.

In recent years, nanotechnology has become pivotal in manipulating biological systems. Nanocomposite hydrogels, intricate molecular networks interwoven with nanoparticles or nanostructures, have gained substantial attention.[11] These composites offer innovative solutions, addressing challenges in tissue regeneration by combining diverse nanoparticles-inorganic/ceramic (hydroxyapatite, silica), polymeric (hyper-branched polyesters, cyclodextrins), metal/metal-oxide (gold, silver), and carbon-based nanomaterials (carbon nanotubes, graphene) - with polymeric networks.[12–14] This strategic fusion yields nanocomposites boasting tailored physical properties and functionalities, revolutionizing advanced biomaterials for tissue engineering and regenerative medicine. For instance, an injectable organic-inorganic nanocomposite GelMA hydrogel system doped Sr-substituted xonotlite (Sr-CSH) nanofibers was developed. This nanocomposite GelMA hydrogel has great potential for bone regeneration.[15]

Despite advancements, reports on the utilization of nanocomposite hydrogels in dentistry, particularly for VPT, remain limited. Bekhouche et al introduced an innovative fibrin nanocomposite hydrogel integrated with clindamycin (CLIN)-loaded Poly (D, L) Lactic Acid (PLA) nanoparticles (NPs), imparting antibacterial properties to the nanocomposite hydrogel. This formulation presents a promising avenue for establishing an aseptic environment conducive to supporting dental pulp reconstruction.[16] Similarly, Han et al developed an electrospun gelatin methacryloyl (GelMA) fibrous scaffold incorporating beta-tricalcium phosphate (TCP) particles for pulp capping. This GelMA/TCP composite demonstrated the capacity to induce the differentiation of odontoblast-like cells capable of secreting dentin matrix in vitro.[17] However, there still remains a significant gap in the comprehensive evaluation of the efficacy that these nanocomposite hydrogels have in VPT. It is crucial to advance the development of novel strategies that holistically address inflammation control and dentin mineralization for efficient VPT in clinical settings.

Calcium phosphate (CaP) boasts a rich history of application in both medical and dental fields owing to its remarkable ability to emulate the mineralized structure of bones and teeth.[18,19] Moreover, CaP has demonstrated prowess in stimulating cell migration and differentiation, rendering it an exceptional bioactive material for regenerative dental therapies.[20–26] Studies have specifically highlighted the capability of CaP nanoparticles (NPs) to induce odontoblast differentiation and enhance calcified tissue formation in controlled in vitro settings.[27] L-arginine (L-Arg) is recognized as a conditionally essential amino acid crucial for the health and maturity of mammals.[28] Studies have shown that L-Arg contributes to the deposition of hydroxyapatite, thereby promoting mineralization.[29–31] Zinc, an essential trace element, plays a pivotal role in managing oxidative stress, growth regulation, and immune function by modulating inflammatory cytokines.[32,33] Research has underscored the healing potential of zinc phosphate (ZnP) as a foundational material in mitigating pulp inflammation.[34] Combining nanoparticles formulated from L-Arg, CaP, and ZnP (L-(CaP-ZnP) NPs) presents an intriguing prospect. Such nanoparticles have the potential to leverage the multifunctional attributes of their individual components, culminating in dual effects - anti-inflammatory properties alongside the promotion of dentin bridge formation.

Sodium alginate (SA) is a widely embraced biodegradable and biocompatible polysaccharide in the pharmaceutical sector. Its versatility lies in its ability to form gels through calcium ion cross-linking (ionotropic gelation process), along with its non-toxic and non-immunogenic traits.[35] SA showcases diverse applications in varied dosage forms, including mucoadhesive systems, microspheres, microcapsules, tablets, and even sutures.[36–40] In order to apply L-(CaP-ZnP) NPs to inflamed pulp, we chose SA hydrogel as the carrier material to load L-(CaP-ZnP) NPs. In this context, we envisioned that a nanocomposite hydrogel, incorporating L-(CaP-ZnP) NPs and SA, could create an optimal microenvironment for efficient VPT through anti-inflammatory and pro-mineralization effects. The present study involved the synthesis of a novel L-arginine modified CaP-ZnP nanoparticles using polyacrylic acid (PAA) as a template, subsequently combined with sodium alginate to form a nanocomposite hydrogel. This formulation was achieved through the cross-linking between calcium and zinc ions in L-(CaP-ZnP) NPs and carboxyl groups within SA. The sustained release of L-Arg and calcium and zinc ions from the L-(CaP-ZnP)/SA nanocomposite hydrogel facilitated odontoblast differentiation and inflammation suppression. Mechanistically, the L-(CaP-ZnP)/SA nanocomposite hydrogel demonstrated the ability to activate the p38 signaling pathway, enhancing the odontogenic differentiation of dental pulp stem cells (DPSCs). This study presents a novel strategy for VPT and the repair of inflamed pulp, contributing valuable insights to the field.

## Materials and Methods
### Materials
Polyacrylic acid (PAA), 1-(3-Dimethylaminopropyl)-3-ethylcarbodiimide hydrochloride (EDC), and N-Hydroxysuccinimide (NHS) were obtained from Sigma-Aldrich (USA). L-Arginine (L-Arg) was purchased from Dalian Meilun Biological Technology Co., Ltd. Zinc oxide (ZnO), calcium hydroxide ($Ca(OH)_2$), sodium hydrogen phosphate ($Na_2HPO_4$), and isopropyl alcohol (IPA) were obtained from Sinopharm Chemical Reagent Beijing Co., Ltd. Sodium alginate (SA) was obtained from Macklin Biochemical Co., Ltd.

## Synthesis of the CaP-ZnP NPs

ZnO (17.5 mg) and $Ca(OH)_2$ (25 mg) were dissolved in deionized water (100 mL) under magnetically stirred and ultrasonic process, respectively. Then, 1mL PAA aqueous solution (0.2 g $mL^{-1}$) was added into the mixed solution and ultrasonically dispersed for 30 min until the transparent solution was obtained. Subsequently, IPA (200 mL) was added dropwise to the above mixed solution under vigorous stirring at room temperature to get Ca-Zn nanospheres. After 30 minutes, $Na_2HPO_4$ (160 mg) was added under vigorous stirring for another 12 hours to get CaP-ZnP NPs, then the resulting precipitate was collected by centrifugation and then washed with water three times to remove the impurities.

## Synthesis of the L-(CaP-ZnP) NPs

EDC (15 mg), NHS (9 mg), and CaP-ZnP NPs (11 mg) were dissolved in deionized water (100 mL) under magnetically stirred and ultrasonic process for 8 hours at room temperature, then 20 mg L-Arg was added to the above mixture under stirring for another 24 hours. The L-(CaP-ZnP) NPs were separated from the mixture by centrifuging and washing with water three times.

## Synthesis of the L-(CaP-ZnP)/SA Nanocomposite Hydrogel

The L-(CaP-ZnP) NPs (500 mg) and SA (72 mg) were added to deionized water (2 mL) and stirred overnight to obtain the L-(CaP-ZnP)/SA nanocomposite hydrogel.

## Characterization

Transmission electron micrographs (TEM) were taken by JEOL-2100F transmission electron microscope under a 200 kV accelerating voltage. Scanning electron microscopy (SEM) images and the energy dispersive X-ray (EDX) spectrum were carried out with a JEOL JSM-7610F scanning electron microscope. The chemical compositions of metal elements in the sample were measured by inductively coupled plasma atomic emission spectrometry (ICP–AES) (Leeman, USA). Fourier transform infrared (FTIR) spectra were obtained using a Nicolet 6700-FTIR spectrometer (Nicolet, USA). Malvern's Zetasizer Nano ZSE Nanoparticle Size and Zeta Potential Analyzer were from the United Kingdom.

## Isolation and Culture of Human Dental Pulp Stem Cells (hDPSCs)

Medical Ethics Committee of Jilin University Stomatological Hospital reviewed and approved the collection of hDPSCs (approval number: 2021[89]). This study was in accordance with the Declaration of Helsinki. Informed consent was obtained from all participants. The ages of patients ranged from 18 to 23 years old. All patients provided written informed consent to participate. Human dental pulp tissue was extracted from premolars and third molars for orthodontic treatment from patients in the Department of Oral and Maxillofacial Surgery at Jilin University Stomatological Hospital. The teeth were required to be intact and free from caries. hDPSCs were isolated from dental pulp tissue using the tissue block enzyme digestion method and cultured in minimal essential medium alpha modification (α-MEM; Hyclone, USA) with 10% fetal bovine serum, 100 U $mL^{-1}$ penicillin, and 100 mg $mL^{-1}$ streptomycin at 37 °C in a 5% $CO_2$ incubator. Cells of passages 3–5 were used for all of the experiments.

## Preparation of Extracts

The method and extraction condition were carried out according to previous studies and the International Organization for Standardization (ISO) method 10993-12: sample preparation and reference Materials. Samples of the L-(CaP-ZnP) /SA nanocomposite hydrogel containing L-(CaP-ZnP) NPs (2 mg) or MTA paste containing MTA (2 mg) were incubated in 1 mL α-MEM at 37 °C in a humidified atmosphere of 95% air with 5% $CO_2$ for 24 h, respectively. The medium was collected by centrifuging at 1000 g for 5 minutes. The collected medium was the extract. The extracts were prepared freshly for each experiment. For cell experiments, the obtained extracts were diluted to (1/2, 1/3, 1/4, 1/5, 1/6, 1/7, and 1/8) with medium.

## Cell Cytotoxicity and Proliferation

The cytotoxicity and proliferation of the L-(CaP-ZnP)/SA nanocomposite hydrogel were evaluated using the cell counting kit (CCK)-8 (Cellcook, China) assay and live/dead staining. In general, hDPSCs were seeded into 96-well plates ($5 \times 10^3$ cells per well) and treated with the L-(CaP-ZnP)/SA nanocomposite hydrogel extract for 24 h, 48 h, and 72 h. After adding CCK-8 to each well, the plates were further incubated for 2 h. The optical density (OD) value was measured at 450 nm by using an Absorbance Microplate Reader (RT-6000; Rayto Life Science and Technology Co, Shenzhen, China). The experiments were carried out in triplicate.

In addition, the viability of hDPSCs was tested with the double fluorescent dye method. hDPSCs were seeded into 24 well plates ($2 \times 10^4$ cells per well) for 24 hours prior to the experiment. Then the cells were treated with the L-(CaP-ZnP)/SA nanocomposite hydrogel extract for 1, 2, and 3 days. After washing the cells with PBS three times, the cells were incubated with green fluorescent dye (Calcein-AM) and red fluorescent dye (PI) for 30 min at 37 °C. The cells subjected to different treatments were investigated using a fluorescence microscope. Each experiment was carried out in triplicate.

## Anti-Inflammation Analysis of the L-(CaP-ZnP)/SA Nanocomposite Hydrogel

RAW 264.7 cells and hDPSCs were used to assess the anti-inflammatory activity. The cells were pre-treated with lipopolysaccharide (LPS), then the culture medium was replaced with the fresh medium containing nanocomposite hydrogel or MTA extract solutions for a duration of 24 h. Following the treatment, the levels of anti-inflammatory cytokine mRNA were analyzed by quantitative real-time polymerase chain reaction (qRT-PCR). The specific primer sequences can be found in Table S1. Each experiment was carried out in triplicate.

## RNA Extraction and qRT-PCR

According to the manual instruction provided with the product, total RNA was extracted with RNAiso Plus (Takara, Beijing, China), and cDNA was prepared applying the Hifair $^®$ III 1st Strand cDNA Synthesis SuperMix (Yeasen, Shanghai, China). QRT-PCR was executed using Hieff$^®$ qPCR SYBR Green Master Mix (Yeasen, Shanghai, China) with 20 μL reaction mixtures on the Bio-Rad CFX Real-Time PCR Detection System. β-actin gene, as a housekeeping gene, was chosen and the expression levels of target genes were estimated by the $2^{-\Delta\Delta Ct}$ method.

## Alkaline Phosphatase (ALP) and Alizarin Red S (ARS) Staining

The hDPSCs were cultured in an osteogenic differentiation medium with LPS and co-cultured with nanocomposite hydrogel or MTA extract solutions. On days 7 and 14, hDPSCs were fixed using 4% paraformaldehyde (PFM) at room temperature for 10–15 minutes. Then, the cells were incubated with the BCIP/NBT ALP staining kit (Beyotime, Shanghai, China) according to the manual instruction. On day 21, the cells were washed with PBS and fixed with PFM. The fixed cells were then stained with ARS solution (Beyotime, Shanghai, China) for 30 min after washing three times with PBS. The stained cells were observed and imaged using an inverted microscope (BX-51, Olympus, Tokyo, Japan) and scanner (Epson V800, Tokyo, Japan). To further identify the role of the p38 signaling pathway in the process of L-(CaP-ZnP)/SA-induced odontogenesis, SB203580 (20 μM) (MCE, Shanghai, China) as a selective inhibitor of p38 was added. Then, the ALP and ARS staining were carried out to explore whether the odontogenic differentiation induced by the L-(CaP-ZnP)/SA nanocomposite hydrogel was inhibited. The experiments were carried out in triplicate.

## QRT-PCR Assay for the Detection of Odontogenic Markers

The hDPSCs were cultivated in 6-well plates at a density of $1 \times 10^5$ cells per well and treated with LPS. Then inflamed hDPSCs were co-cultured with nanocomposite hydrogel or MTA extract solutions. The total RNA of DPSCs was extracted on days 7 and 14 and the expression levels of DSPP, DMP1, BSP, ALP, Runx2, and OPN were evaluated by the method described earlier. The specific primer sequences can be found in Table S1. Each experiment was carried out in triplicate.

## Protein Preparation and Western Blot Analysis

The hDPSCs were seeded in a 6-well plate at $1\times10^5$ cells per well and then were treated with LPS. Cells were cultured for 7 days in osteogenic differentiation medium with nanocomposite hydrogel or MTA extract solutions. The hDPSCs were lysed by RIPA lysis buffer comprising protease and phosphatase inhibitors (Beyotime, Shanghai, China), and centrifuged at 14800 rpm for 20 min at 4 °C, and supernatants were isolated. Then the protein concentrations were quantified using the BCA kit (Beyotime, Shanghai, China). Protein samples were mixed with loading buffer and then heated for 10 min at 98 °C. Equal amounts of protein were electrophoresed on 10% polyacrylamide gels, followed by transfer into PVDF membrane (Millipore, Billerica, USA). After blockage with 5% non-fat dry milk in TBST buffer, the following primary antibodies were used: p38 (1:1000, Beyotime, Shanghai, China), p-p38 (1:1000, Beyotime, Shanghai, China) Runx2 (1:1000, ABclonal, Wuhan, China) and β-actin (1:20000, Proteintech, Wuhan, China). PVDF membranes were incubated with primary antibodies and peroxidase-conjugated secondary antibodies (1:10000 dilution), respectively. Chemiluminescence was examined using a sensitive ECL detection kit (Proteintech, Wuhan, China) and bands were analyzed by a ChemiDoc Imaging system (Tanon, Shanghai, China). Each experiment was carried out in triplicate.

## Immunofluorescence Staining

The hDPSCs were seeded at a density of $4\times10^3$ cells per well in a 12-well plate, then treated with LPS. The cells were cultured in an osteogenic differentiation medium with nanocomposite hydrogel or MTA extracts solutions for 7 days. Following this step, hDPSCs were fixed in 4% paraformaldehyde for 15 minutes at 4 °C. After washing with PBS three times, the cells were blocked in an Immunol Staining Blocking Buffer (Beyotime, Shanghai, China) at room temperature for 1 h. hDPSCs were then incubated overnight at 4 °C with Runx2 (rabbit polyclonal antibody, 1:200, ABclonal, Wuhan, China). Subsequently, the cells were treated with an Alexa Fluor 555-labeled Donkey Anti-rabbit IgG (H+L) secondary antibody (1:500, Beyotime, Shanghai, China). 4′,6-diamidino-2-phenylindole (DAPI, Sigma-Aldrich, St Louis, MO) were used to stain the nucleus. Finally, the fluorescence-positive cells were observed and imaged using a fluorescence microscope (Olympus DP70, Tokyo, Japan). The experiments were carried out in triplicate.

## Animal Experiments

All animal experiments were conducted on the basis of the Guidelines for the Care and Use of Laboratory Animals of Institutional Animal Care and Use Committee of Changchun Institute of Applied Chemistry Chinese Academy of Sciences (20220102). All experiments involving animals followed the ARRIVE guidelines. Forty-five male Wistar rats (7 weeks old) were obtained from Liaoning Changsheng Biotechnology Co., Ltd. The rats were housed in a controlled environment at 22 °C and 60% humidity with a 12-hour light-dark cycle. After a one-week acclimatization period, a total of 45 rats were randomly divided into three groups (n=15). Briefly, we anesthetized the rats and then established the model of early-stage pulpitis as described previously.[41] Each rat was fastened and 0.5% povidone-iodine was used to disinfect the oral cavity and maxillary first molar. Subsequently, we used a high-speed turbine tooth drill bur (BR49, ISO001008) with a terminal diameter of 0.5 mm to prepare cavities with 1.0 mm depth. The dental pulp was exposed by gently stabbing with a sterile 40# K file through cavities. The exposed dental pulp was rinsed with normal saline and then treated with sterile cotton balls soaked in 1 μg mL$^{-1}$ of Escherichia coli LPS for 15 min. The L-(CaP-ZnP)/SA nanocomposite hydrogel or MTA (Dentsply Endodontics, USA) was used in the cavity of the first molar to cover the exposed pulp. The coronal cavity was then sealed using Fuji IX glass-ionomer cement (GC, Japan).

On days 3, 7, and 28, the rats were euthanized. The specimens were fixed and decalcified using 10% ethylenedia-minetetraacetic acid (EDTA, BBI) for 60 days. Fixed specimens were sectioned into 3 μm sections and stained with hematoxylin and eosin (HE) staining. The specimens were examined with immunohistochemistry to evaluate the level of inflammation and the expressions of differentiation markers. The primary antibodies used were TNF-α (1:500, Bioss, Beijing, China), IL-1β (1:500, Bioss, Beijing, China), and Runx2 (1:200, ABclonal, Wuhan, China). The staining slices were observed and imaged with a microscope (Olympus DP74, Tokyo, Japan).

## Statistical Analysis

The data were expressed as mean ± standard deviation (SD). Statistical analysis was carried out using Student's *t*-test or one-way analysis of variance (ANOVA) and P value < 0.05 was considered statistically significant.

## Results and Discussion

### Characterization and Biocompatibility of the L-(CaP-ZnP)/SA Nanocomposite Hydrogel

A novel L-(CaP-ZnP)/SA nanocomposite hydrogel was synthesised. Initially, polyacrylic acid (PAA) was blended with Zinc oxide (ZnO) and calcium hydroxide (Ca(OH)$_2$) to create the PAA-Ca/Zn complex, acting as a template through the interaction between carboxyl groups in PAA and Ca as well as Zn ions. Subsequently, isopropyl alcohol (IPA) was added dropwise into the solution, resulting in the formation of Ca-Zn nanoparticles (NPs) measuring approximately 200 nm (Figure 1A). After a 30-minute interval, sodium hydrogen phosphate (Na$_2$HPO$_4$), functioning as the phosphate anion source, was added to facilitate the production of CaP-ZnP NPs. Additionally, the addition of L-Arg to the activated CaP-ZnP NPs led to the creation of uniformly dispersed L-(CaP-ZnP) NPs, approximately 200 nm in diameter (Figures 1B and S1). Finally, the L-(CaP-ZnP) NPs were mixed into a sodium alginate solution (SA) to formulate the L-(CaP-ZnP)/SA nanocomposite hydrogel. As depicted in Figure S2, an Eppendorf (EP) tube containing the SA hydrogel or the L-(CaP-ZnP)/SA nanocomposite hydrogel was inverted and placed at room temperature. Remarkably, after 10 minutes, while the SA hydrogel flowed downward, the L-(CaP-ZnP)/SA nanocomposite hydrogel remained at the bottom of the EP tube. This observation indicated that the incorporation of L-(CaP-ZnP) NPs heightened the viscosity of the nanocomposite hydrogel, enhancing its ability to effectively seal exposed dental pulp. The gelation process could be attributed to the interaction between the calcium and zinc ions from L-(CaP-ZnP) NPs and the carboxyl groups within SA. The L-(CaP-ZnP) NPs not only offer stable cross-linking sites on their surface, but also enable a sustained release of calcium and zinc ions for the ionotropic gelation process with SA, thereby ensuring the long-term structural integrity of the nanocomposite hydrogel.

The scanning electron microscopy (SEM) image displayed the rough surface of the L-(CaP-ZnP)/SA nanocomposite hydrogel, featuring scattered granular protrusions (Figure 1C). Elemental distribution analysis of the L-(CaP-ZnP) NPs revealed the presence of expected elements including C, N, O, Ca, Zn, and P (Figure 1D). The chemical composition of the CaP-ZnP NPs was determined by inductively coupled plasma atomic emission spectrometry (ICP-AES), confirming that the content of Ca and Zn is 6.13 wt% and 8.51wt%, respectively (Figure 1E). The Fourier transform infrared (FTIR) spectra (Figure 1F) exhibited vibrational absorption peaks at 1620 cm$^{-1}$ (C=N bond) and 1330 cm$^{-1}$ (C-N bond) in the L-(CaP-ZnP) NPs spectra, validating successful attachment of L-Arg to CaP-ZnP NPs. Additionally, characteristic peaks of SA were evident at 1600 cm$^{-1}$, 1410 cm$^{-1}$, and 1030 cm$^{-1}$, attributed to asymmetric and symmetric telescopic vibrations of COO, and the telescopic vibration of C-O, respectively, in the L-(CaP-ZnP)/SA spectra. The L-(CaP-ZnP)/SA spectra mainly reflected the characteristic absorption peaks of SA, possibly due to the low content of L-Arg. Furthermore, a significant change in zeta potential between CaP-ZnP NPs and L-(CaP-ZnP) NPs was observed during the preparation process, indicating the successful modification of the nanoparticles (Figure 1G).

To evaluate the cytotoxicity of the L-(CaP-ZnP)/SA nanocomposite hydrogel on human dental pulp stem cells (hDPSCs), various dilutions (1/2, 1/3, 1/4, 1/5, 1/6, 1/7, and 1/8) of the L-(CaP-ZnP)/SA nanocomposite hydrogel extract were used to culture hDPSCs for 24 hours. The cell counting kit-8 (CCK-8) assay revealed that the 1/3 dilution of the L-(CaP-ZnP)/SA nanocomposite hydrogel extract notably enhanced cell proliferation (Figure S3). Consequently, the 1/3 dilution was selected for subsequent experiments. The biocompatibility of the L-(CaP-ZnP)/SA nanocomposite hydrogel was further evaluated using CCK-8 and Live/dead staining. As depicted in Figure 1H, CCK-8 analysis demonstrated robust growth of hDPSCs treated with the L-(CaP-ZnP)/SA nanocomposite hydrogel extract, exhibiting higher proliferation rates than the control group on days 1, 2, and 3. The Live/dead staining exhibited numerous live cells (stained green) following treatment with the L-(CaP-ZnP)/SA nanocomposite hydrogel, indicating comparable or improved viability compared to the control group (Figure 1I). Moreover, the density of live cells exhibited a time-dependent trend on days 1, 2, and 3. These findings collectively affirm the excellent biocompatibility and proliferation-inducing properties of the L-(CaP-ZnP)/SA nanocomposite hydrogel, underscoring its potential for various biological applications.
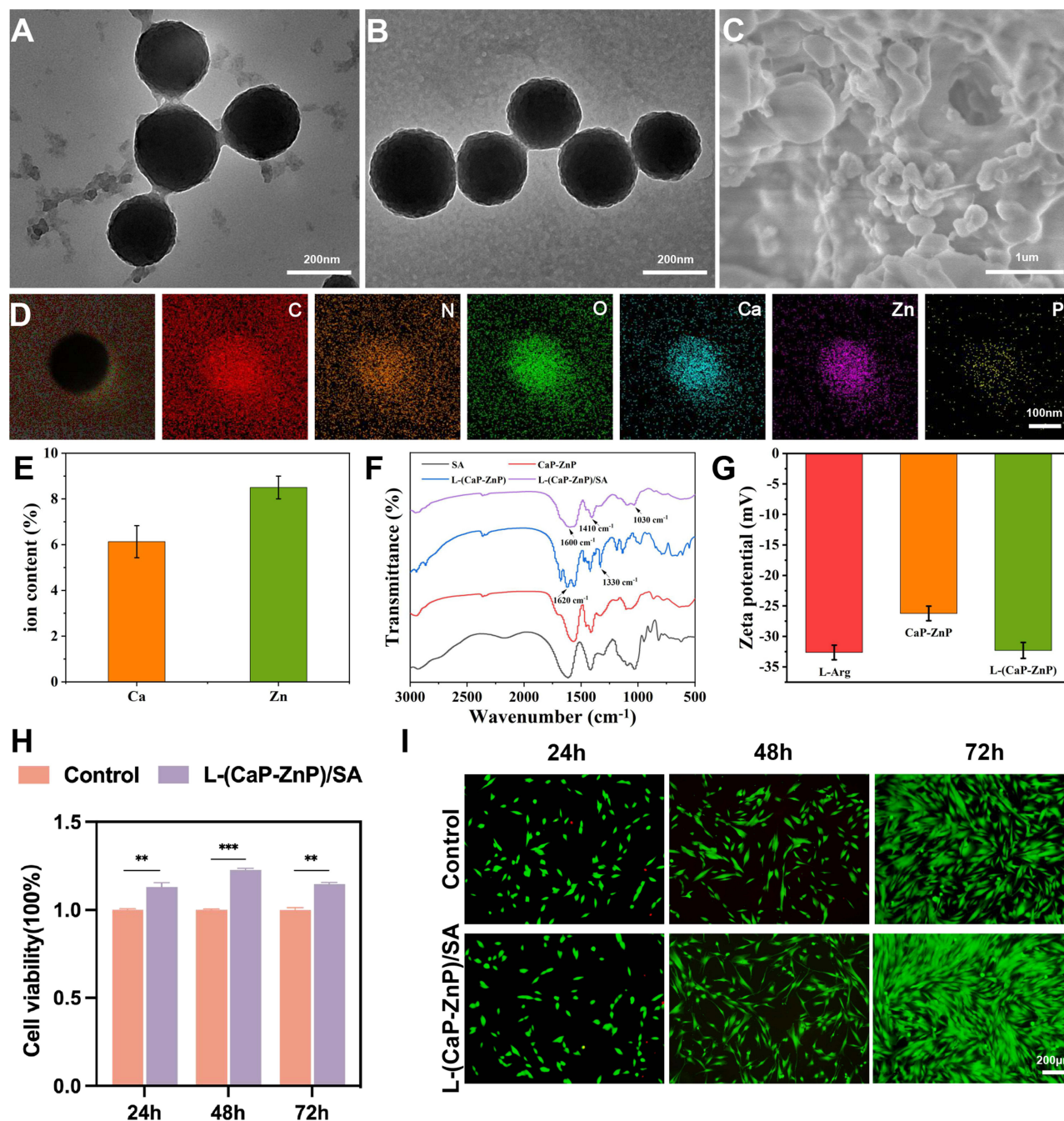
**Figure 1** Characterization and Biocompatibility of the L-(CaP-ZnP)/SA nanocomposite hydrogel. TEM images of (**A**) Ca-Zn NPs. (**B**) L-(CaP-ZnP) NPs. (**C**) SEM image of L-(CaP-ZnP)/SA nanocomposite hydrogel. (**D**) The elemental mapping images of L-(CaP-ZnP) NPs. (**E**) The content of Ca and Zn in CaP-ZnP NPs. (**F**) FTIR spectra of SA (black), CaP-ZnP NPs (red), L-(CaP-ZnP) NPs (blue), and L-(CaP-ZnP)/SA nanocomposite hydrogel (purple). (**G**) Zeta potential of CaP-ZnP NPs and L-(CaP-ZnP) NPs. (**H**) hDPSCs viability after incubation with the L-(CaP-ZnP)/SA nanocomposite hydrogel extract for 1, 2, and 3 days. (**I**) Fluorescence images of hDPSCs stained with Calcein-AM /PI after treatment with L-(CaP-ZnP)/SA nanocomposite hydrogel extract for 1, 2, and 3 days. Statistical analysis is performed by *t*-test in this section. Error bars represent mean ± standard deviation. Asterisks indicate statistically significant differences (**P < 0.01, and ***P <0.001).

## Anti-Inflammatory Properties of the L-(CaP-ZnP)/SA Nanocomposite Hydrogel in vitro

The pulp-dentin complex serves as a critical physiological structure involved in dentin and pulp development. Upon exposure to bacteria or their toxic secretions, various cell types within the pulp-dentin complex, including dental pulp stem cells, macrophages, and other immune cells, detect invading bacteria by expressing pattern recognition

receptors.[42,43] This triggers the release of proinflammatory mediators such as tumor necrosis factor α (TNF-α), inter-leukin (IL)-1β, IL-6, and IL-10, leading to recruitment of immune cells and initiating early inflammatory responses aimed at eliminating invading microorganisms.[44–46] However, sustained inflammation resulting from antimicrobial activities can cause irreversible damage to dental pulp tissue, ultimately leading to complete pulpal necrosis.[43] Reducing inflammation is pivotal for dental pulp healing, especially considering that lipopolysaccharide (LPS) stands as a primary cause of pulpitis. To assess the anti-inflammatory effects of the L-(CaP-ZnP)/SA nanocomposite hydrogel, hDPSCs were pretreated with LPS and subsequently cultured in the presence or absence of the L-(CaP-ZnP)/SA nanocomposite hydrogel extract or MTA extract for 24 hours. The application of LPS notably increased the expression of pro-inflammatory cytokine genes (TNF-α, IL-1β, and IL-6) as determined by quantitative real-time polymerase chain reaction (qRT-PCR). In contrast, the L-(CaP-ZnP)/SA nanocomposite hydrogel demonstrated significant downregulation of IL-1β, IL-6, and TNF-α expression, while MTA exhibited limited inhibition of these cytokines (Figure 2A). Consequently, under inflammatory conditions, the L-(CaP-ZnP)/SA nanocomposite hydrogel exhibited markedly superior anti-inflammatory capabilities compared to MTA.

During pulpitis, recruited macrophages possess the capacity to differentiate into two distinct phenotypes: the pro-inflammatory M1 phenotype, characterized by TNF-α, IL-1β, and IL-6 expression, and the anti-inflammatory M2 phenotype, known for expressing IL-10 and Arg-1. This transition from M1 to M2 phenotypes plays a pivotal role in mitigating an excessive inflammatory response.[47] To further assess the anti-inflammatory potential of the L-(CaP-ZnP)
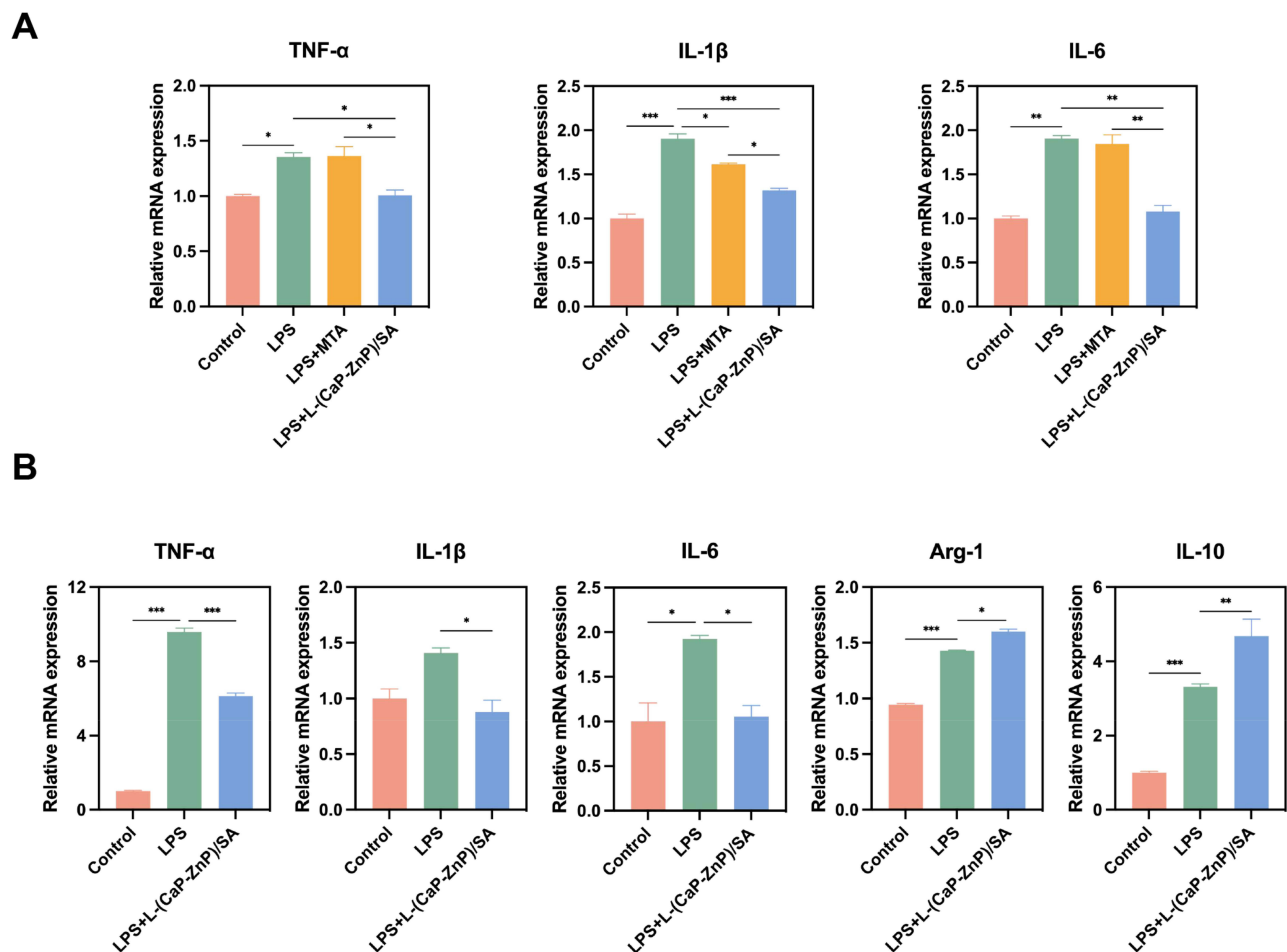


**Figure 2** Assessment of Anti-inflammatory Properties of L-(CaP-ZnP)/SA Nanocomposite Hydrogel in vitro. (**A**) hDPSCs were cultured with L-(CaP-ZnP)/SA nanocomposite hydrogel or MTA extract in the presence of LPS for 24h. The expression of TNF-α, IL-1β, and IL-6 was determined by qRT-PCR. (**B**) Raw264.7 cells were cultured with L-(CaP-ZnP)/SA nanocomposite hydrogel or MTA extract in the presence of LPS for 24h. The expression of TNF-α, IL-1β, IL-6, Arg-1, and IL-10 was determined by qRT-PCR. Statistical analysis is performed by one-way ANOVA. Error bars represent mean ± standard deviation. Asterisks indicate statistically significant differences (*P < 0.05, **P < 0.01, and ***P < 0.001).

/SA nanocomposite hydrogel, the macrophages were cultured in the presence of LPS to mimic an inflammatory microenvironment. Figure 2B illustrated a notable elevation in the expression of M1-related inflammatory cytokines (TNF-α, IL-6, and IL-1β) in response to LPS stimulation. Significantly, the levels of M1-related biomarkers notably decreased in the L-(CaP- ZnP)/SA group compared to the LPS group. Moreover, the L-(CaP-ZnP)/SA group exhibited augmented levels of M2-related biomarkers compared to the LPS group. Collectively, these findings highlight the substantial anti-inflammatory effects of the L-(CaP-ZnP)/SA nanocomposite hydrogel in an in vitro setting.

## Effects of the L-(CaP-ZnP)/SA Nanocomposite Hydrogel on the Mineralization and Odontogenic Differentiation Under Inflammatory Conditions in vitro

DPSCs represent the predominant cell type within the dental pulp and play a pivotal role in the generation of reparative dentin within the pulp-dentin complex. Upon injury to the dental pulp, DPSCs migrate to the affected area where they undergo differentiation into odontoblast-like cells, initiating reparative dentin formation and instigating the pulp repair process.[48] hDPSCs were subjected to treatment with the L-(CaP-ZnP)/SA nanocomposite hydrogel in the presence of LPS to assess its odontogenic potential. The alkaline phosphatase (ALP) staining images showed that LPS suppressed the ALP activity of hDPSCs and the L-(CaP-ZnP)/SA nanocomposite hydrogel dramatically improved the ALP activity of LPS-stimulated hDPSCs compared with MTA on day 7 (Figure 3A and B). This enhancement trend persisted on day 14 (Figure 3C and D), indicating the superior potential of the L-(CaP-ZnP)/SA nanocomposite hydrogel over MTA in promoting odontogenic activity in hDPSCs under inflammatory conditions. Additionally, Alizarin red S (ARS) staining demonstrated reduced calcium nodules in the LPS group compared to the control group on day 21. Remarkably, the L-(CaP-ZnP)/SA nanocomposite hydrogel and MTA significantly facilitated calcium nodule formation in the presence of LPS. Notably, the L-(CaP-ZnP)/SA nanocomposite hydrogel exhibited greater effectiveness in promoting calcium nodule formation compared to MTA (Figure 3E and F). These findings provide further evidence supporting the ability of the L-(CaP-ZnP)/SA nanocomposite hydrogel to induce odontogenesis in DPSCs under inflammatory conditions. The qRT-PCR was employed to measure the expression of genes associated with odontogenesis. These included dentin sialopho-sphoprotein (DSPP), dental matrix protein 1 (DMP1), bone sialoprotein (BSP), alkaline phosphatase (ALP), recombinant runt-related transcription factor 2 (Runx2), and osteopontin (OPN). Overall, these proteins play pivotal roles in stimulating cell differentiation and facilitating dentin mineralization. Runx2 is crucial in both the secretion and miner-alization of the dentin matrix during tooth development.[49,50] As illustrated in Figure 3G and H, on days 7 and 14, exposure to LPS significantly diminished the expression of these genes. Remarkably, the L-(CaP-ZnP)/SA nanocompo-site hydrogel demonstrated an increased expression of all these genes. In contrast, the MTA group did not exhibit significant recovery in gene expression levels. Therefore, the qRT-PCR data suggests that under inflammatory conditions, the L-(CaP-ZnP)/SA nanocomposite hydrogel can drive odontogenesis in hDPSCs by upregulating the expression of these odontogenic genes.

The Western blot (WB) assay and Immunofluorescence (IF) staining were employed to analyze the expression of the odontogenic-related protein, Runx2. As depicted in Figure 4A and B, after a 7-day culture period, there was a reduction in the levels of Runx2 within the LPS-exposed group, indicating the inhibitory effect of LPS on odontogenesis. Notably, when compared to the LPS group, the presence of the L-(CaP-ZnP)/SA nanocomposite hydrogel significantly elevated the Runx2 levels, whereas MTA exhibited a marginal increase in Runx2 expression. Additionally, the immunofluorescence staining images of Runx2 revealed lower fluorescence intensities in LPS-induced hDPSCs compared to the control group. Consistent with the Western blot findings, the fluorescence intensities notably increased in the L-(CaP-ZnP)/SA group in contrast to the LPS group. Conversely, the MTA group exhibited only a marginal increase in fluorescence intensities (Figures 4C and S4). These collective findings suggest that the L-(CaP-ZnP)/SA nanocomposite hydrogel might facilitate greater odontogenic differentiation in vitro compared to MTA. Similarly, Zhao et al reported CNPs/DMP1-loaded self-assembly hydrogel possessed potential promotion on dentinogenic differentiation. Nevertheless, this study did not compare the efficacy of hydrogel with MTA, which is the most commonly used repair material in clinical practice, and lacked studies investigating the relevant mechanisms.[51]
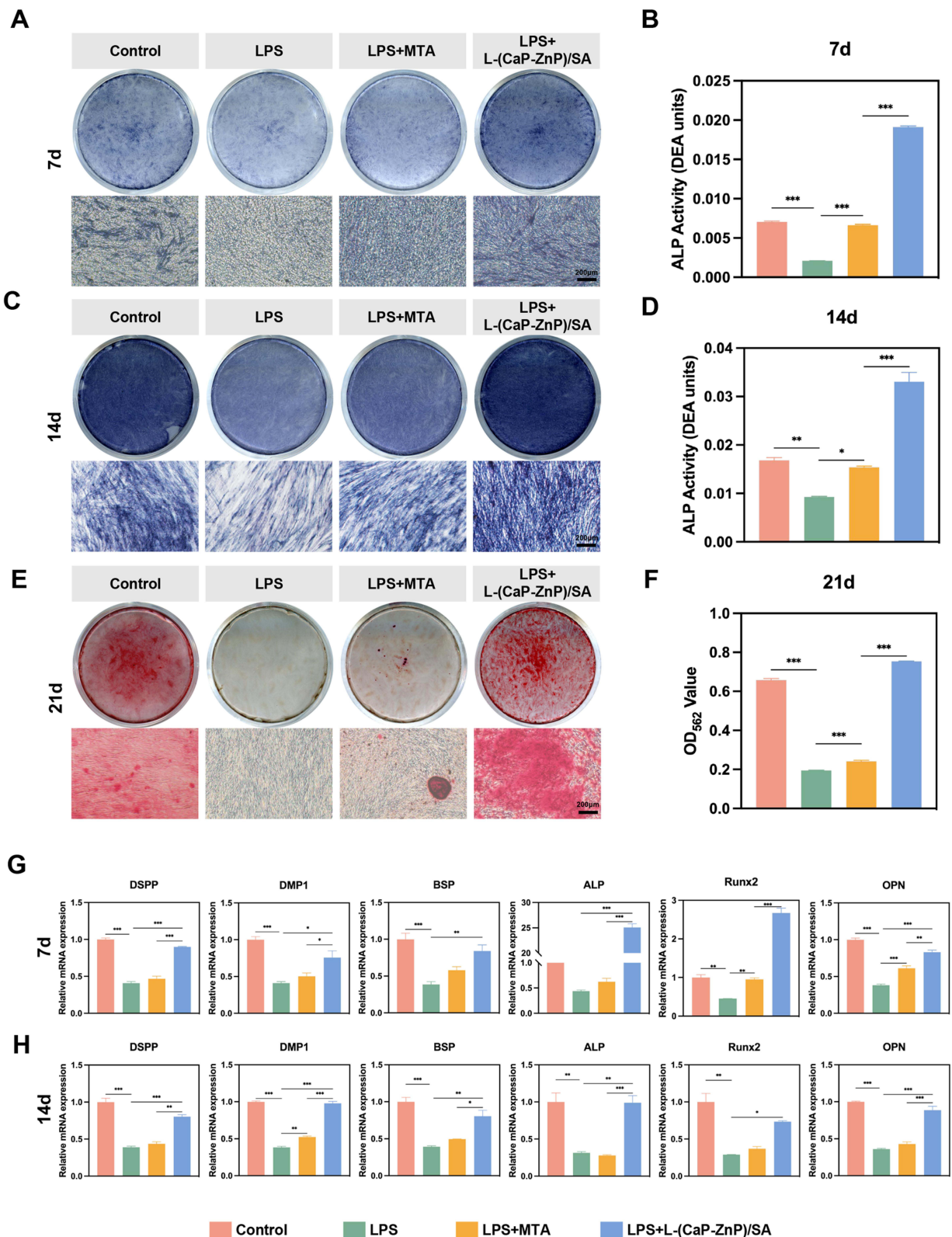
**Figure 3** Effects of the L-(CaP-ZnP)/SA nanocomposite hydrogel on odonto/osteogenic differentiation in LPS-stimulated hDPSCs. (**A–D**) Staining and quantitative detection of ALP activity on days 7 and 14. (**E** and **F**) ARS staining and quantitative detection on day 21. (**G** and **H**) Relative gene expression levels of DSPP, DMP1, BSP, ALP, Runx2, and OPN of hDPSCs after culture in the L-(CaP-ZnP)/SA nanocomposite hydrogel or MTA extract with LPS treated for 7 and 14 days. Error bars represent mean ± standard deviation. Statistical analysis is performed by one-way ANOVA. Asterisks indicate statistically significant differences (*$P < 0.05$, **$P < 0.01$, and ***$P < 0.001$).
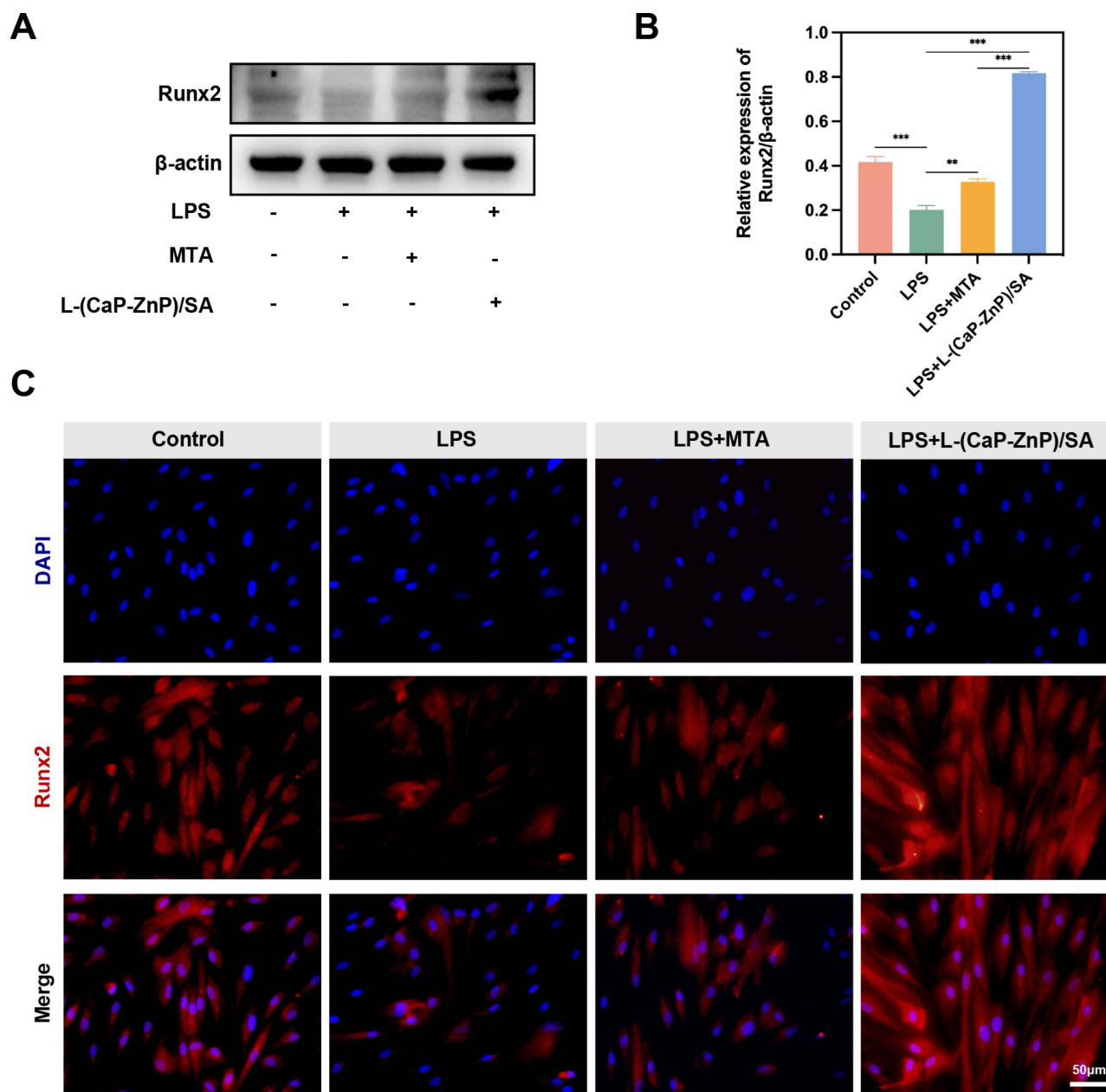
**Figure 4** WB and IF reveal odontogenic effects of the L-(CaP-ZnP)/SA nanocomposite hydrogel. (**A** and **B**) Western blot and semiquantitative assessment displaying the expression of the odontogenic-related protein (Runx2) on day 7. (**C**) Immunofluorescence staining of Runx2 on day 7. Abbreviations: "+" and "–" represent "with" and "without", respectively. Error bars represent mean ± standard deviation. Statistical analysis is performed by one-way ANOVA. Asterisks indicate statistically significant differences (**P < 0.01, and ***P < 0.001).

## Activation of the p38 Signaling Pathway Contributes to L-(CaP-ZnP)/SA-Induced Odontogenesis Under Inflammatory Conditions

Having demonstrated the ability of the L-(CaP-ZnP)/SA nanocomposite hydrogel to induce odontogenic differentiation, our subsequent investigation aimed to uncover the potential underlying mechanisms governing this process. Previous studies have highlighted the significance of the p38 signaling pathway in fundamental cellular activities, encompassing proliferation, differentiation, motility, and cell survival.[52,53] Moreover, research has indicated the advantageous role of the p38 signaling pathway in facilitating dental pulp stem cell migration and dentinogenesis.[54,55] Nevertheless, scant literature exists regarding the influence of the p38 signaling pathway on the odontogenic differentiation capacity of DPSCs under inflammatory conditions. Hence, we conducted a WB assay to investigate the involvement of the p38

signaling pathway as a potential mechanism underlying the induction of odontogenesis by the L-(CaP-ZnP)/SA nanocomposite hydrogel under inflammatory conditions. As illustrated in Figures 5A and S5A, LPS exhibited a downregulating effect on the phosphorylated p38 levels compared to the control group. However, this impact was effectively reversed upon application of the L-(CaP-ZnP)/SA nanocomposite hydrogel. These findings suggest that the L-(CaP-ZnP)/SA nanocomposite hydrogel can effectively activate the p38 signaling pathway under inflammatory conditions.

For an in-depth exploration of whether the p38 activation contributed to L-(CaP-ZnP)/SA-induced odontogenesis under inflammatory conditions, SB203580, an inhibitor of the p38 signaling pathway, was utilized to obstruct this pathway. As depicted in Figures 5B and S5B, the phosphorylated p38 expression was notably suppressed upon pretreatment with SB203580 in the L-(CaP-ZnP)/SA group under LPS condition. Subsequently, ALP staining, ARS staining, qRT-PCR, WB, and IF staining were further conducted to assess the odontogenic effects of L-(CaP-ZnP)/SA nanocomposite hydrogel under the inhibition of SB203580. The ALP activity, as depicted in Figure 5C, showed a substantial reduction under the inhibition of SB203580 in the L-(CaP-ZnP)/SA group after 7 days of incubation. A similar trend was observed on day 14 (Figure 5D). ARS staining revealed a significant reduction in mineralized nodules on day 21 (Figure 5E). Additionally, the qRT-PCR results illustrated a substantial decrease in odontogenic gene expressions, including DSPP, DMP1, and Runx2, under inflammatory conditions upon blocking the p38 signaling pathway with SB203580 (Figure 5F). Further, Western blot analysis showed a significant decline in the Runx2 level under the SB203580 and LPS condition (Figures 5G and S5C). Consistent with the Western blot findings, the fluorescence intensity of Runx2 also notably decreased with the inhibition of SB203580 (Figures 5H and S6). In summary, our study suggests that the activation of the p38 signaling pathway contributes to L-(CaP-ZnP)/SA-induced odontogenesis under inflammatory conditions. This mechanism may involve nanoparticles released by the L-(CaP-ZnP)/SA nanocomposite hydrogel activating $Ca^{2+}$/calmodulin-dependent kinase II (CaMK II). Previous reports have linked CaMK II to osteogenic or odontogenic differentiation,[56] and its activation could trigger p38 phosphorylation.[57] However, the in-depth mechanisms require further investigation.

## The L-(CaP-ZnP)/SA Nanocomposite Hydrogel Efficiently Promotes Inflammation Resolution and Enhances Dentin Mineralization in vivo

To evaluate the potential application of L-(CaP-ZnP)/SA nanocomposite hydrogel for enhancing inflammatory dental pulp repair and inducing pulp-dentin complex generation, a pulpitis model was established in Wistar rats (Figure 6A). The progression of pulpitis was evaluated at various time points over 28 days post-operation. Hematoxylin and eosin (HE) staining (Figure 6B) revealed that by day 3, the coronal pulp in the control and MTA groups displayed diffuse infiltration by numerous inflammatory cells. In contrast, the L-(CaP-ZnP)/SA group exhibited mild inflammatory infiltration, relatively limited in distribution. By day 7, significant infiltrations of inflammatory cells persisted in the control and MTA groups, leading to continued dental pulp tissue destruction extending towards the root pulp. However, a marked reduction in inflammatory cells was evident in the L-(CaP-ZnP)/SA group.

To further investigate the impact of the L-(CaP-ZnP)/SA nanocomposite hydrogel on tissue inflammation, we conducted immunohistochemistry (IHC) staining to evaluate the expression of two crucial pro-inflammatory cytokines, tumor necrosis factor-alpha (TNF-α), and interleukin 1-beta (IL-1β). These cytokines play pivotal roles in initiating the inflammatory response, potentially causing damage to dental pulp tissue.[58] Our study revealed a significant reduction in the expression of these inflammatory factors within the L-(CaP-ZnP)/SA group compared to the control and MTA groups by day 3. Particularly after seven days of model establishment and treatment, there was a remarkable decrease in TNF-α-positive and IL-1β-positive cell infiltrates within the L-(CaP-ZnP)/SA group. Conversely, considerable levels of TNF-α-positive and IL-1β-positive cells were still evident in the control and MTA groups (Figure 6C). These findings suggest that the L-(CaP-ZnP)/SA nanocomposite hydrogel effectively alleviates the inflammatory response. Its anti-inflammatory properties provide a conducive immune microenvironment for repairing inflamed pulp tissue.

On day 28, both the control and MTA groups exhibited complete degeneration and necrosis of the dental pulp. Remarkably, substantial restorative dentin was evident in the L-(CaP-ZnP)/SA group. Additionally, odontoblast-like cells
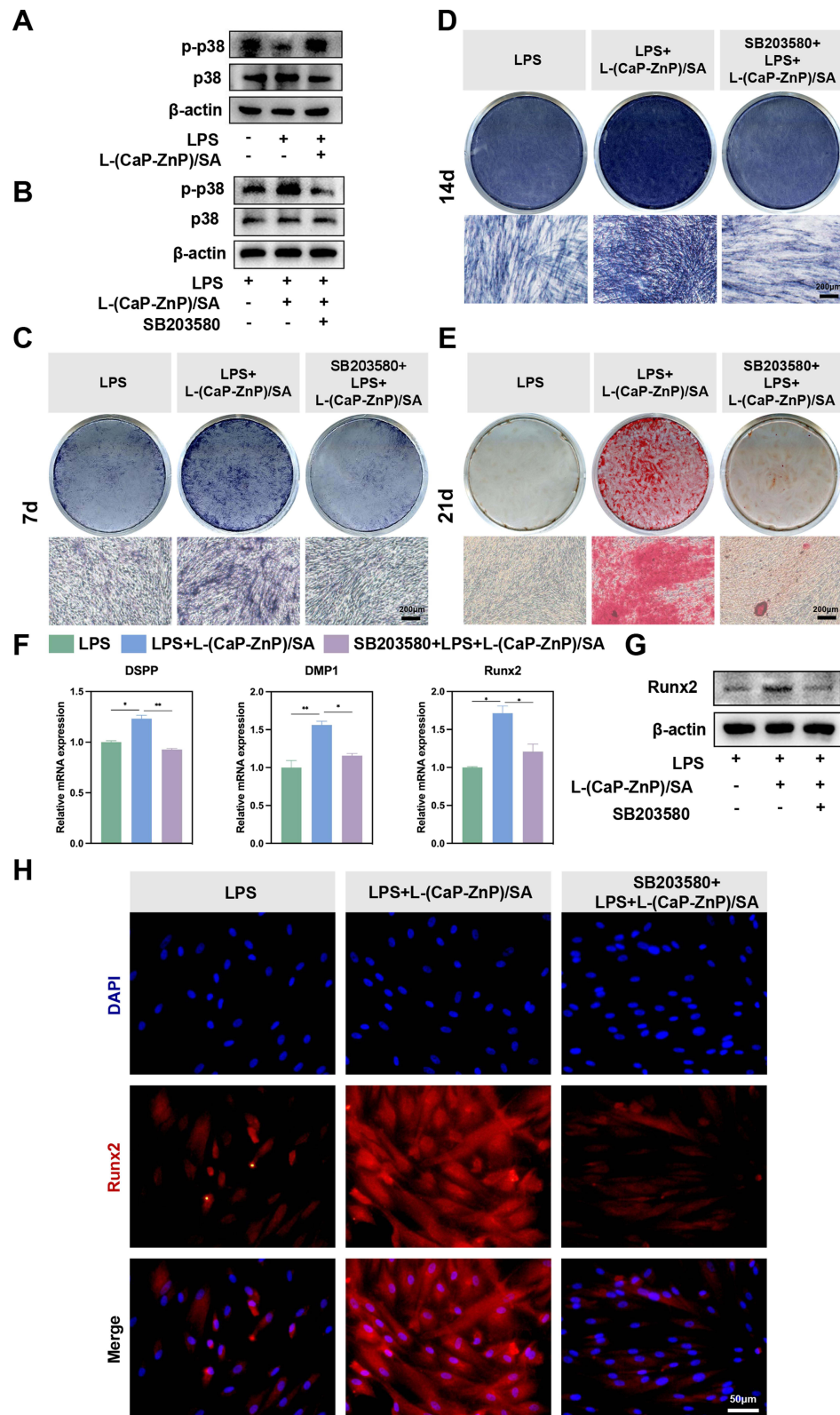
**Figure 5** The L-(CaP-ZnP)/SA nanocomposite hydrogel stimulated odontogenesis by activating the p38 signaling pathway in LPS-stimulated hDPSCs. (**A**) Western blot analysis depicted the expression of p-p38 and p38 proteins in LPS-stimulated hDPSCs treated with or without the L-(CaP-ZnP)/SA nanocomposite hydrogel for 7 days. (**B**) Western blot analysis exhibited the expression of p-p38 and p38 proteins in LPS-stimulated hDPSCs pretreated with or without SB203580 (20 μM) for 24 hours, followed by culturing with the L-(CaP-ZnP)/SA nanocomposite hydrogel for 7 days. (**C** and **D**) ALP staining on days 7 and 14. (**E**) ARS staining on day 21. (**F**) Relative gene expression levels of DSPP, DMP1, and Runx2 on day 7. (**G**) Effects of SB203580 on odontogenesis induced by the L-(CaP-ZnP)/SA nanocomposite hydrogel in LPS-stimulated hDPSCs. (**H**) Immunofluorescence staining of Runx2 on day 7. Abbreviations: "+" and "−" symbols represent "with" and "without", respectively. Error bars indicate mean ± standard deviation. Statistical analysis is performed by one-way ANOVA. Asterisks indicate statistically significant differences (*$P < 0.05$, and **$P < 0.01$).
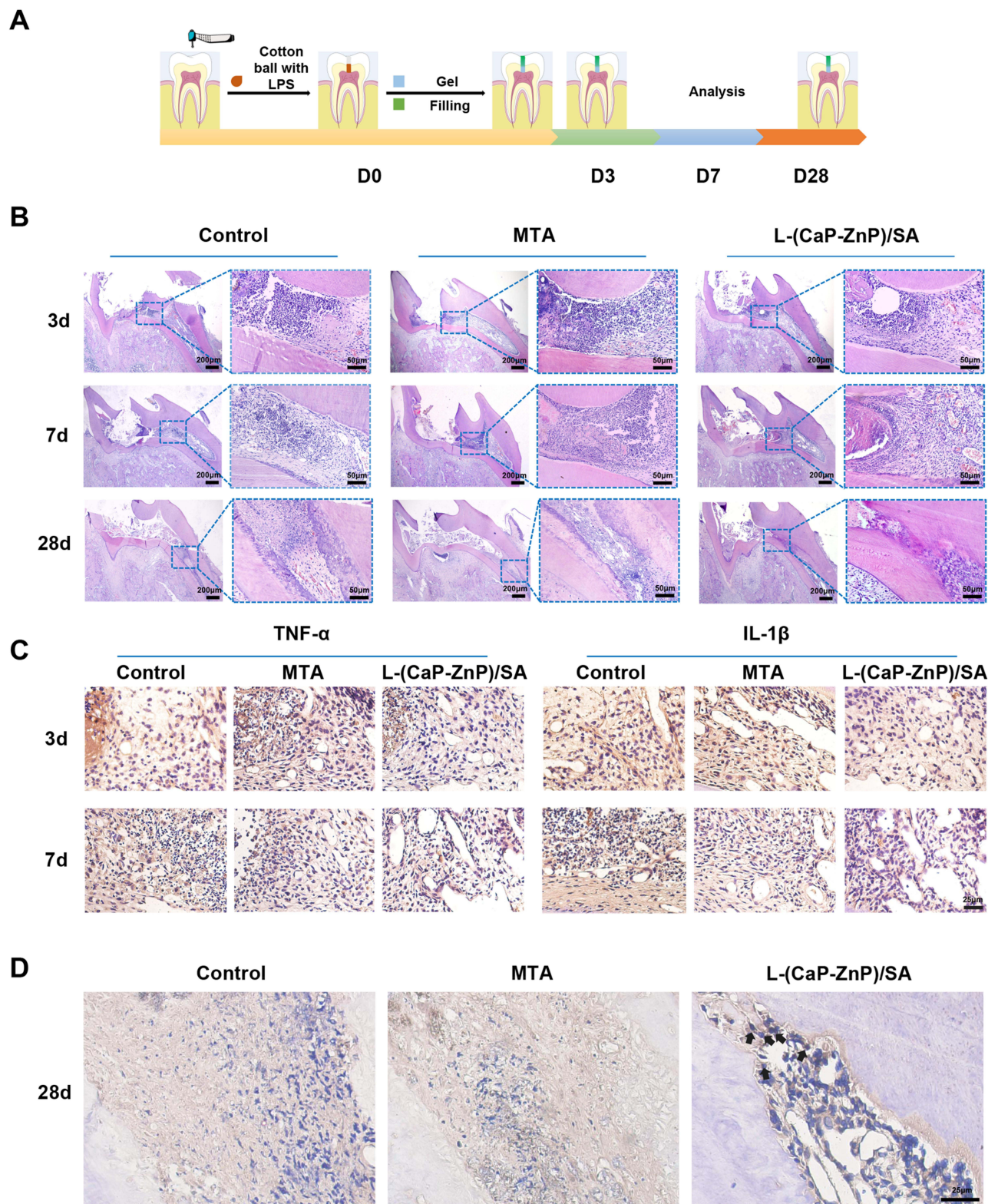
**Figure 6** Effects of the L-(CaP-ZnP)/SA Nanocomposite Hydrogel on Pulpitis in a Rat Model. (**A**) Schematic depiction illustrating the process of establishing pulpitis. (**B**) Hematoxylin and eosin (HE) staining. (**C**) Immunohistochemical staining displaying TNF-α and IL-1β. (**D**) Immunohistochemical staining showing Runx2. Positive signals are indicated by black arrows.

exhibited a polarized morphology, forming a distinct palisade layer around the newly formed dentin bridges (Figure 6B). Notably, the root pulp remained intact. To assess the differentiation potential of DPSCs following pulp capping, IHC was utilized to evaluate the expression of Runx2, a mineralization marker. In the L-(CaP-ZnP)/SA group, robust Runx2 immunoreactivity was observed in the outer pulp area, where odontoblast-like cells were adjacent to the dentin-like layer (Figure 6D). In contrast, the degenerated pulp tissue of the control and MTA groups exhibited only faint immunoreactivity. Overall, the L-(CaP-ZnP)/SA nanocomposite hydrogel demonstrates significant promise in inflammation resolution and dentin mineralization in vivo. Similarly, Han et al developed a GelMA/TCP nanocomposite scaffold showing the therapeutic efficacy in promoting in vivo hard tissue formation. However, this nanocomposite scaffold exhibited a relatively limited functionality, lacking anti-inflammatory effects, whereas the resolution of inflammation is crucial for vital pulp preservation.[43,59]

## Conclusion

In summary, we have developed L-(CaP-ZnP)/SA nanocomposite hydrogel for the treatment of pulpitis in a rat model. The L-(CaP-ZnP)/SA nanocomposite hydrogel is easily prepared by mixing L-(CaP-ZnP) NPs with SA. The L-(CaP-ZnP)/SA nanocomposite hydrogel with excellent biocompatibility shows promising dual functionality, exhibiting both robust anti-inflammatory properties and significant potential for dentin mineralization in vitro and in vivo. The anti-inflammatory capabilities of the nanocomposite hydrogel provided a conducive environment for the repair of inflamed pulp tissue, while its ability to stimulate dentin formation presented promising prospects for pulp preservation. More importantly, we delved into the underlying mechanisms conducive to the restoration of inflamed dental pulp, an area less investigated in prior study. We found that the p38 signaling pathway contributed to L-(CaP-ZnP)/SA nanocomposite hydrogel-induced osteogenesis under inflammatory conditions. However, the specific mechanisms by which the p38 signaling pathway promotes odontogenesis require further investigation. The multifaceted functionality of the L-(CaP-ZnP)/SA nanocomposite hydrogel holds considerable promise in the realm of VPT. Further studies to explore its long-term effects, safety profile, and clinical applicability are warranted for its potential translation into dental therapeutics aimed at efficient pulp tissue preservation and regeneration. Furthermore, prior to clinical translational application, simplifying the preparation process of L-(CaP-ZnP)/SA nanocomposite hydrogel may be considered to facilitate large-scale production.

## Acknowledgments

## Disclosure

The authors report no conflicts of interest in this work.

## References

1. Huang GTJ. Dental pulp and dentin tissue engineering and regeneration advancement and challenge. *Front Biosci*. 2011;E3(2):788–800. doi:10.2741/e286
2. Aguilar P, Linsuwanont P. Vital pulp therapy in vital permanent teeth with cariously exposed pulp: a systematic review. *J Endodontics*. 2011;37 (5):581–587. doi:10.1016/j.joen.2010.12.004
3. Siddiqui Z, Acevedo-Jake AM, Griffith A, et al. Cells and material-based strategies for regenerative endodontics. *Bioact Mater*. 2022;14:234–249. doi:10.1016/j.bioactmat.2021.11.015
4. Morotomi T, Washio A, Kitamura C. Current and future options for dental pulp therapy. *Japan Dent Sci Rev*. 2019;55(1):5–11. doi:10.1016/j. jdsr.2018.09.001
5. Tziafas D, Smith AJ, Lesot H. Designing new treatment strategies in vital pulp therapy. *J Dent*. 2000;28(2):77–92. doi:10.1016/S0300-5712(99) 00047-0

6. Duncan HF. Present status and future directions—Vital pulp treatment and pulp preservation strategies. *Int Endodontic J*. 2022;55(S3):497–511. doi:10.1111/iej.13688

7. Kunert M, Lukomska-Szymanska M. Bio-inductive materials in direct and indirect pulp capping—a review article. *Materials*. 2020;13(5):1204. doi:10.3390/ma13051204

8. Torabinejad M, Hong C, Mcdonald F, Pittford T. Physical and chemical properties of a new root-end filling material. *J Endodontics*. 1995;21 (7):349–353. doi:10.1016/S0099-2399(06)80967-2

9. Holland R, De Souza V, Nery MJ, Otoboni Filho JA, Bernabé PFE, Dezan E. Reaction of rat connective tissue to implanted dentin tubes filled with mineral trioxide aggregate or calcium hydroxide. *J Endodontics*. 1999;25(3):161–166. doi:10.1016/S0099-2399(99)80134-4

10. Kim DH, Jang JH, Lee BN, et al. Anti-inflammatory and mineralization effects of ProRoot MTA and endocem MTA in studies of human and rat dental pulps in vitro and in vivo. *J Endodontics*. 2018;44(10):1534–1541. doi:10.1016/j.joen.2018.07.012

11. Merino S, Martín C, Kostarelos K, Prato M, Vázquez E. Nanocomposite hydrogels: 3D polymer–nanoparticle synergies for on-demand drug delivery. *ACS Nano*. 2015;9(5):4686–4697. doi:10.1021/acsnano.5b01433

12. Jiang L, Jiang B, Xu J, Wang T. Preparation of pH-responsive oxidized regenerated cellulose hydrogels compounded with nano-ZnO/chitosan/ aminocyclodextrin ibuprofen complex for wound dressing. *Int J Biol Macromol*. 2023;253:126628. doi:10.1016/j.ijbiomac.2023.126628

13. Huang S, Hong X, Zhao M, et al. Nanocomposite hydrogels for biomedical applications. *Bioeng Transla Med*. 2022;7(3):e10315. doi:10.1002/ btm2.10315

14. Chen W, Ming Y, Wang M, et al. Nanocomposite hydrogels in regenerative medicine: applications and challenges. *Macromol Rapid Commun*. 2023;44(15):2300128. doi:10.1002/marc.202300128

15. Yu X, Wang X, Li D, et al. Mechanically reinforced injectable bioactive nanocomposite hydrogels for in-situ bone regeneration. *Chem Eng J*. 2022;433:132799. doi:10.1016/j.cej.2021.132799

16. Bekhouche M, Bolon M, Charriaud F, et al. Development of an antibacterial nanocomposite hydrogel for human dental pulp engineering. *J Mater Chem B*. 2020;8(36):8422–8432. doi:10.1039/D0TB00989J

17. Han Y, Dal-Fabbro R, Mahmoud AH, et al. GelMA/TCP nanocomposite scaffold for vital pulp therapy. *Acta Biomater*. 2023:S1742706123006529. doi:10.1016/j.actbio.2023.11.005

18. Palmer I, Nelson J, Schatton W, Dunne NJ, Buchanan F, Clarke SA. Biocompatibility of calcium phosphate bone cement with optimised mechanical properties: an in vivo study. *J Mater Sci Mater Med*. 2016;27(12):191. doi:10.1007/s10856-016-5806-2

19. Eliaz N, Metoki N. Calcium phosphate bioceramics: a review of their history, structure, properties, coating technologies and biomedical applications. *Materials*. 2017;10(4):334. doi:10.3390/ma10040334

20. Lin Y, Huang S, Zou R, et al. Calcium phosphate cement scaffold with stem cell co-culture and prevascularization for dental and craniofacial bone tissue engineering. *Den Mater*. 2019;35(7):1031–1041. doi:10.1016/j.dental.2019.04.009

21. AbdulQader ST, Kannan TP, Rahman IA, Ismail H, Mahmood Z. Effect of different calcium phosphate scaffold ratios on odontogenic differentia- tion of human dental pulp cells. *Mater Sci Eng C*. 2015;49:225–233. doi:10.1016/j.msec.2014.12.070

22. Wang L, Zhang C, Li C, et al. Injectable calcium phosphate with hydrogel fibers encapsulating induced pluripotent, dental pulp and bone marrow stem cells for bone repair. *Mater Sci Eng C*. 2016;69:1125–1136. doi:10.1016/j.msec.2016.08.019

23. Zakaria MN, Cahyanto A, El-Ghannam A. Basic properties of novel bioactive cement based on silica-calcium phosphate composite and carbonate apatite. *KEM*. 2016;720:147–152. doi:10.4028/www.scientific.net/KEM.720.147

24. Eslaminejad MB, Bordbar S, Nazarian H. Odontogenic differentiation of dental pulp-derived stem cells on tricalcium phosphate scaffolds. *J Dent Sci*. 2013;8(3):306–313. doi:10.1016/j.jds.2013.03.005

25. Lee SK, Lee SK, Lee SI, et al. Effect of calcium phosphate cements on growth and odontoblastic differentiation in human dental pulp cells. *J Endodontics*. 2010;36(9):1537–1542. doi:10.1016/j.joen.2010.04.027

26. Qin W, Chen JY, Guo J, et al. Novel calcium phosphate cement with metformin-loaded chitosan for odontogenic differentiation of human dental pulp cells. *Stem Cells Int*. 2018;2018:1–10. doi:10.1155/2018/7173481

27. Mahran AH, Fahmy SH, Ibrahim SS. Evaluation of stem cell differentiation medicated with calcium phosphate nanoparticles in chlorohexidine paste. *Bull Natl Res Cent*. 2023;47(1):37. doi:10.1186/s42269-023-01011-2

28. Tsikas D, Wu G. Homoarginine, arginine, and relatives: analysis, metabolism, transport, physiology, and pathology. *Amino Acids*. 2015;47 (9):1697–1702. doi:10.1007/s00726-015-2055-5

29. Tan X, Xue Z, Zhu H, Wang X, Xu D. How charged amino acids regulate nucleation of biomimetic hydroxyapatite nanoparticles on the surface of collagen mimetic peptides: molecular dynamics and free energy investigations. *Cryst Growth Des*. 2020;20(7):4561–4572. doi:10.1021/acs. cgd.0c00353

30. Marwah N, Asokan S, Puranik MP, et al. Arginine: a New Paradigm in Preventive Oral Care. *Int J Clin Pediatr Dent*. 2023;16(5):698–706. doi:10.5005/jp-journals-10005-2693

31. Konagala RK, Mandava J, Anwarullah A, Uppalapati LV, Karumuri S, Angadala PL. Synergistic effect of arginine on remineralization potential of fluoride varnish and nanohydroxyapatite on artificial caries lesions: an in vitro study. *J Contemp Dent Pract*. 2020;21(9):1048–1053. doi:10.5005/ jp-journals-10024-2915

32. Prasad AS. Zinc: role in immunity, oxidative stress and chronic inflammation. *Curr Opin Clin Nutr Metab Care*. 2009;12(6):646–652. doi:10.1097/ MCO.0b013e3283312956

33. Tsou TC, Chao HR, Yeh SC, Tsai FY, Lin HJ. Zinc induces chemokine and inflammatory cytokine release from human promonocytes. *J Hazard Mater*. 2011;S0304389411011356. doi:10.1016/j.jhazmat.2011.09.035

34. Lervik T. The effect of zinc phosphate and carboxylate cements on the healing of experimentally induced pulpitis. *Oral Surg Oral Med Oral Pathol*. 1978;45(1):123–130. doi:10.1016/0030-4220(78)90235-9

35. Jadach B, Świetlik W, Froelich A. Sodium alginate as a pharmaceutical excipient: novel applications of a well-known polymer. *J Pharmaceut Sci*. 2022;111(5):1250–1261. doi:10.1016/j.xphs.2021.12.024

36. Xing Y, Qing X, Xia H, et al. Injectable hydrogel based on modified gelatin and sodium alginate for soft-tissue adhesive. *Front Chem*. 2021;9:744099. doi:10.3389/fchem.2021.744099

37. Sagdicoglu Celep AG, Demirkaya A, Solak EK. Antioxidant and anticancer activities of gallic acid loaded sodium alginate microspheres on colon cancer. *Curr Appl Phys*. 2022;40:30–42. doi:10.1016/j.cap.2020.06.002

38. Chen M, Hu Y, Zhou J, et al. Facile fabrication of tea tree oil-loaded antibacterial microcapsules by complex coacervation of sodium alginate/quaternary ammonium salt of chitosan. *RSC Adv.* 2016;6(16):13032–13039. doi:10.1039/C5RA26052C

39. Ito I, Ito A, Unezaki S. Investigation of oral preparation that is expected to improve medication administration: preparation and evaluation of oral gelling tablet using sodium alginate. *YAKUGAKU ZASSHI.* 2017;137(8):969–977. doi:10.1248/yakushi.16-00261

40. De La Harpe KM, Marimuthu T, Kondiah PPD, Kumar P, Ubanako P, Choonara YE. Synthesis of a novel monofilament bioabsorbable suture for biomedical applications. *J Biomed Mater Res.* 2022;110(10):2189–2210. doi:10.1002/jbm.b.35069

41. Zhu N, Chatzistavrou X, Papagerakis P, Ge L, Qin M, Wang Y. Silver-doped bioactive glass/chitosan hydrogel with potential application in dental pulp repair. *ACS Biomater Sci Eng.* 2019;5(9):4624–4633. doi:10.1021/acsbiomaterials.9b00811

42. Cooper PR, Takahashi Y, Graham LW, Simon S, Imazato S, Smith AJ. Inflammation–regeneration interplay in the dentine–pulp complex. *J Dent.* 2010;38(9):687–697. doi:10.1016/j.jdent.2010.05.016

43. Cooper PR, Holder MJ, Smith AJ. Inflammation and regeneration in the dentin-pulp complex: a double-edged sword. *J Endodontics.* 2014;40(4):S46–S51. doi:10.1016/j.joen.2014.01.021

44. Cooper PR, Chicca IJ, Holder MJ, Milward MR. Inflammation and regeneration in the dentin-pulp complex: net gain or net loss? *J Endodontics.* 2017;43(9):S87–S94. doi:10.1016/j.joen.2017.06.011

45. Staquet MJ, Carrouel F, Keller JF, et al. Pattern-recognition Receptors in Pulp Defense. *Adv Dent Res.* 2011;23(3):296–301. doi:10.1177/0022034511405390

46. Lee SI, Kang SK, Jung HJ, Chun YH, Kwon YD, Kim EC. Muramyl dipeptide activates human beta defensin 2 and pro-inflammatory mediators through Toll-like receptors and NLRP3 inflammasomes in human dental pulp cells. *Clin Oral Invest.* 2015;19(6):1419–1428. doi:10.1007/s00784-014-1361-8

47. Guo D, Dong W, Cong Y, et al. LIF aggravates pulpitis by promoting inflammatory response in macrophages. *Inflammation.* 2023;47(1):307–322. doi:10.1007/s10753-023-01910-6

48. Liao C, Wang Y, Ou Y, Wu Y, Zhou Y, Liang S. Effects of sclerostin on lipopolysaccharide-induced inflammatory phenotype in human odontoblasts and dental pulp cells. *Int J Biochem Cell Biol.* 2019;117:105628. doi:10.1016/j.biocel.2019.105628

49. Qiu Y, Saito T. Novel bioactive adhesive monomer CMET promotes odontogenic differentiation and dentin regeneration. *IJMS.* 2021;22(23):12728. doi:10.3390/ijms222312728

50. Gronthos S, Brahim J, Li W, et al. Stem cell properties of human dental pulp stem cells. *J Dent Res.* 2002;81(8):531–535. doi:10.1177/154405910208100806

51. Zhao Y, Song L, Li M, et al. Injectable CNPs/DMP1-loaded self-assembly hydrogel regulating inflammation of dental pulp stem cells for dentin regeneration. *Mater Today Bio.* 2024;24:100907. doi:10.1016/j.mtbio.2023.100907

52. Roux PP, Blenis J. ERK and p38 MAPK-activated protein kinases: a family of protein kinases with diverse biological functions. *Microbiol Mol Biol Rev.* 2004;68(2):320–344. doi:10.1128/MMBR.68.2.320-344.2004

53. Cuadrado A, Nebreda AR. Mechanisms and functions of p38 MAPK signalling. *Biochem J.* 2010;429(3):403–417. doi:10.1042/BJ20100323

54. Lew WZ, Feng SW, Lin CT, Huang HM. Use of 0.4-Tesla static magnetic field to promote reparative dentine formation of dental pulp stem cells through activation of p38 MAPK signalling pathway. *Int Endodontic J.* 2019;52(1):28–43. doi:10.1111/iej.12962

55. Na J, Zhang L, Zheng L, et al. Static magnetic field regulates proliferation, migration, and differentiation of human dental pulp stem cells by MAPK pathway. *Cytotechnology.* 2022;74(3):395–405. doi:10.1007/s10616-022-00533-3

56. Rong J, Pool B, Zhu M, et al. Basic calcium phosphate crystals induce osteoarthritis-associated changes in phenotype markers in primary human chondrocytes by a calcium/calmodulin kinase 2-dependent mechanism. *Calcif Tissue Int.* 2019;104(3):331–343. doi:10.1007/s00223-018-0494-1

57. Wei Y, Jin Z, Zhang H, Piao S, Lu J, Bai L. The transient receptor potential channel, vanilloid 5, induces chondrocyte apoptosis via Ca2+ CaMKII–dependent MAPK and Akt/ mTOR pathways in a rat osteoarthritis model. *Cell Physiol Biochem.* 2018;51(5):2309–2323. doi:10.1159/000495874

58. Hui T, P A, Zhao Y, Yang J, Ye L, Wang C. EZH2 regulates dental pulp inflammation by direct effect on inflammatory factors. *Arch Oral Biol.* 2018;85:16–22. doi:10.1016/j.archoralbio.2017.10.004

59. Han Y, Dal-Fabbro R, Mahmoud AH, et al. GelMA/TCP nanocomposite scaffold for vital pulp therapy. *Acta Biomater.* 2024;173:495–508. doi:10.1016/j.actbio.2023.11.005